Civil and Environmental Engineering
Vol. 21, Issue 2, 936-943, DOI: 10.2478/cee-2025-0071

APPLICATION OF CASTIGLIANO'S THEOREM IN THE ANALYSIS OF SEMI-CIRCULAR ARCH DEFLECTION

Roman HERDA[1,*], Thomas COSGROVE[2], Filip GURKALO[3], Miloš SLIVANSKÝ[1], Jaroslav SANDANUS[1]

[1] Department of Steel and Timber Structures, Slovak University of Technology, Bratislava, Slovakia.
[2] School of Engineering, University of Limerick, Ireland.
[3] Henan Polytechnic University, Henan, China.
[*] corresponding author: roman.herda@stuba.sk

Abstract

The article presents an analytical solution for determining the vertical deformation of a three-hinged arch subjected to a point load at its apex. The theoretical approach is grounded in Castigliano's theorem and utilizes the principle of superposition of strain energy along the arch. A parametric study is included, examining various curvature radius-to-beam thickness ratios to assess when the contributions of strain energy from shear and axial forces must be considered. The parametric study is based on varying the ratio R/h, which ranges from a value of 100 to 0.25. The findings are validated through finite element analysis (FEA) computational models and experimental measurements.

Keywords:

Castigliano´s Theorem;
Deflection;
Three-hinged Arch;
Strain Energy;
Semi-circle.

1 Introduction

For the calculation of deflections in curved beams, Castigliano's theorem, based on the principle of strain energy, can be utilized. In practice, a common scenario involves curved beams where the cross-sectional dimensions are small compared to the radius of curvature. In cases of analysing curved beams with a high R/h ratio, the vertical deformation of the curved beam can be calculated using a formula derived from the strain energy predominantly caused by bending moments. The analytical expression for vertical deformation caused primarily by the bending moment for straight and curved beams is presented in [1].

For engineering practice, it is important to understand the significance and contribution of other internal forces to the overall deformation, and therefore, the article provides an analytical solution for calculating the vertical deformation at the apex of a curved beam, including cases where the R/h ratio is low, requiring the contribution of strain energy induced by axial and shear forces to be considered. The threshold at which axial and shear forces become significant is determined from a parametric study using finite element models. The result of the parametric study highlights the significance of individual internal forces depending on the R/h ratio. The theoretical study is also validated through experimental measurements conducted under laboratory conditions at the University of Limerick in Ireland.

2 Castigliano´s teorem

According to [2], Castigliano's theorem can be applied to calculate deflections in structures when the principle of superposition is valid, and the structural behaviour is linearly elastic. The capabilities of materials for elastic deformation based on their material properties are described in studies [3, 4, 5]. Additionally, a critical condition is that the expression for strain energy must be a function of the applied loads rather than displacements. When these conditions are met, the vertical deformation can be determined using Castigliano's theorem:

$$\delta = \frac{dU}{dP_i}, \tag{1}$$

where:
U - strain energy,
P - load,
δ - resulting deflection of the structure.

According to [6], the magnitude of strain energy, including all acting internal forces as well as the interaction between axial force and bending moment, can be expressed as follows:

$$U = \int\left(\frac{M^2}{2EI} + \frac{N^2}{2AE} - \frac{MN}{RAE} + \frac{\alpha Q^2}{2AG}\right)ds, \tag{2}$$

where:
M, N, Q - internal forces,
A - cross sectional area,
E - Young´s modulus,
G - Shear modulus,
α - Timoshenko shear coefficient,
I - moment of inertia.

In bending within the plane of curvature, as noted by [7-8], each cross-section will experience an axial force N, a shear force Q, and a bending moment M. The aim of the presented study is to evaluate, based on Equation (2), the percentage contribution of all these internal forces to the vertical deflection of a three-hinged semi-circular arch subjected to a point load at its apex.

3 The theoretical solution for three-hinged arch

The analytical solution for the vertical deflection at the apex of a semi-circular arch is developed for a three-hinged arch with a point load at the apex. The geometry of the arch (Fig. 1) is described using polar coordinates for half of the span, considering symmetry.

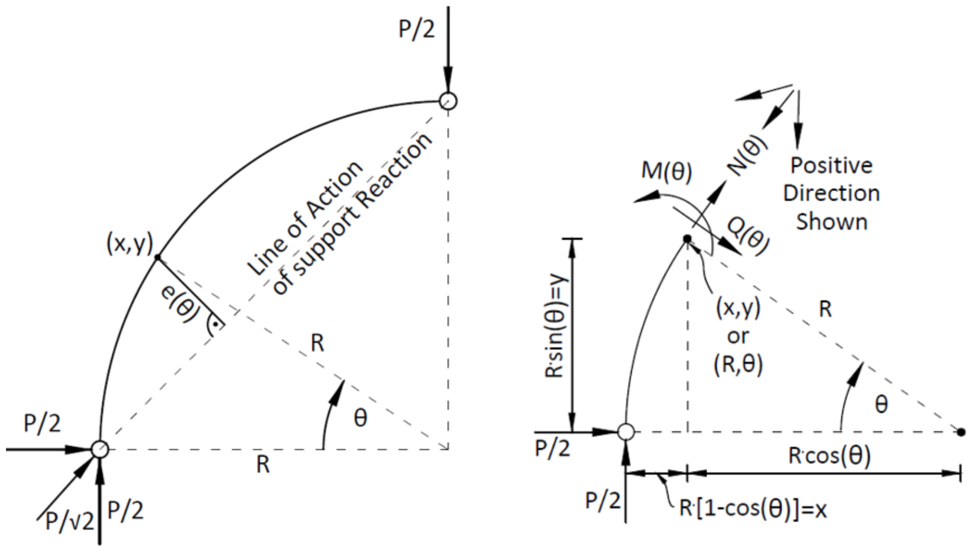

Fig. 1: The geometry of a three-hinged arch subjected to a point load at its apex can be described in polar coordinates.

Based on the given geometry, the internal force magnitudes can be expressed in polar coordinates using equations (3), (4), and (5).

$$M = \frac{PR}{2}(1 - Cos(\theta) - Sin(\theta)), \tag{3}$$

$$N = \frac{-P}{2}(Sin(\theta) + Cos(\theta)), \tag{4}$$

$$Q = \frac{P}{2}(Sin(\theta) - Cos(\theta)), \tag{5}$$

where:
R - radius of the circle,
θ - angular coordinate.

By substituting the expressions (2), (3), (4), and (5) into equation (1), it is possible to define the relationship for calculating the vertical deflection:

$$\delta = \frac{dU}{dP_i} = \frac{d}{dP_i} 2 \cdot \left[\int_0^{\frac{\pi}{2}} \left(\frac{M^2}{2EI} + \frac{N^2}{2AE} - \frac{MN}{RAE} + \frac{\alpha Q^2}{2AG}\right) R d\theta\right] = 2 \cdot \left[\frac{PR^3(\pi-3)}{4EI} + \frac{PR(\pi+2)}{8AE} - \frac{PR(\pi-2)}{8AE} + \frac{\alpha PR(\pi-2)}{8AG}\right], \tag{6}$$

Considering the symmetric nature of the semi-circular three-hinged arch subjected to a load at its apex, it is sufficient to solve the integral equations for only half of the arch, from the support to the apex. To account for the other half of the structure, the final solution must be multiplied by a factor of 2. The limits of the integral are also derived from the conditions of symmetry. By substituting equations (3), (4), and (5) into equation (2), applying the corresponding integral limits, and differentiating the resulting expression for strain energy with respect to the applied load, we obtain an analytical solution for the vertical deflection of the three-hinged semi-circular arch.

The first term in the solution presented in equation (6) represents the contribution of the bending moment to the total deflection at the apex. The second term accounts for the effect of axial forces. The third term captures the interaction between the bending moment and the axial force, while the final term represents the contribution of shear force to the total vertical deformation.

Boresi [9], in his study, notes that when the bending moment M and the axial force N have the same sign, the resulting expression for the inter-action term becomes negative. In typical cases, the strain energy contribution from the interaction term is very small and, in many instances, negative. Based on the conclusions presented in [9], it is recommended to disregard the interaction term in the equation if its value is negative. This simplification is justified because the negative interaction term often has a negligible impact on the overall strain energy and deformation.

Based on the presented arguments and the negative result of the interaction term between the bending moment and the axial force, this term is neglected in further calculations in the article for verifying experimental measurements and validating the parametric study.

4 Parametric study

Based on the geometry of the three-hinged arch (Fig. 1) and Equation (6), a parametric study was conducted for various ratios of the radius of curvature (R) to the section height (h), ranging from 100 to 0.25. The accuracy of the theoretical results derived using Castigliano's theorem was verified through finite element analysis models. For the tested ratios, the following material properties were assumed: Young's modulus E = 210 GPa, Poisson's ratio v = 0.28, shear coefficient for rectangular sections α = 1.2, and a constant cross-sectional width was maintained. Additionally, the same load was applied to all models.

For the comparison of theoretical solution results, multiple models based on the finite element method were developed. The models were created using brick volumetric elements, and the results were subsequently verified using beam models. The volume-element based model was implemented as a contact problem in Abaqus, with hinged boundary conditions (Fig. 2) modelled to reflect the experimental validation described in Section 5. The approximate global size of mesh seeds was determined through a convergence test, resulting in a value of 1 mm. Further mesh refinement did not lead to a significant increase in accuracy.

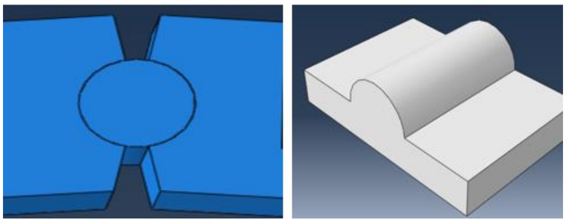

Fig. 2: The boundary conditions of the FEA model with the allowance of rotation at the apex and at the support locations of the three-hinged arch.

Table 1: Results of the parametric study and the percentage contribution of internal forces.

R/h	Theory [mm]	FEA model [mm]	Discrepancy [%]	Bending moment [%]	Axial Force [%]	Shear Force [%]
100	2.02E+02	2.02E+02	0.002	99.97	0.02	0.01
33.333	7.51E+00	7.51E+00	0.000	99.77	0.14	0.09
20	1.63E+00	1.63E+00	-0.002	99.36	0.38	0.26
10	2.07E-01	2.07E-01	0.002	97.51	1.48	1.02
8	1.08E-01	1.08E-01	-0.001	96.16	2.27	1.57
6.667	6.34E-02	6.34E-02	0.000	94.56	3.22	2.22
5.714	4.07E-02	4.07E-02	-0.001	92.73	4.30	2.97
5	2.79E-02	2.79E-02	-0.001	90.72	5.49	3.79
4	1.50E-02	1.50E-02	-0.001	86.22	8.15	5.63
2.857	6.20E-03	6.20E-03	-0.001	76.14	14.11	9.75
2	2.654E-03	2.654E-03	0.012	60.99	23.07	15.94
1.333	1.170E-03	1.170E-03	0.018	41.00	34.89	24.10
1	7.203E-04	7.200E-04	0.046	28.10	42.52	29.37
0.800	5.180E-04	5.180E-04	0.002	20.01	47.31	32.68
0.667	4.053E-04	4.050E-04	0.075	14.80	50.39	34.81
0.571	3.338E-04	3.340E-04	-0.067	11.32	52.45	36.23
0.5	2.843E-04	2.840E-04	0.110	8.90	53.88	37.22
0.444	2.480E-04	2.480E-04	0.002	7.17	54.91	37.93
0.4	2.202E-04	2.200E-04	0.077	5.89	55.66	38.45
0.364	1.981E-04	1.980E-04	0.056	4.91	56.24	38.85
0.333	1.802E-04	1.800E-04	0.099	4.16	56.68	39.15
0.308	1.653E-04	1.650E-04	0.179	3.57	57.03	39.40
0.286	1.527E-04	1.530E-04	-0.174	3.09	57.32	39.59
0.267	1.420E-04	1.420E-04	-0.011	2.70	57.55	39.75
0.25	1.327E-04	1.330E-04	-0.244	2.38	57.73	39.88

The maximum recorded discrepancy between the results of the FEA models and the theoretical solution was just 0.24 %, confirming the high reliability of the analytical approach. Tab. 1 presents the percentage contributions of internal forces affecting the resulting vertical deformation at the apex of the arch under a concentrated load applied at the apex. These contributions are shown as a function of the R/h ratio. Based on the data in the graphical representation in Fig. 3, it can be observed that as the R/h ratio decreases, the influence of axial and shear forces on the total deformation of the semi-circular arch increases significantly.

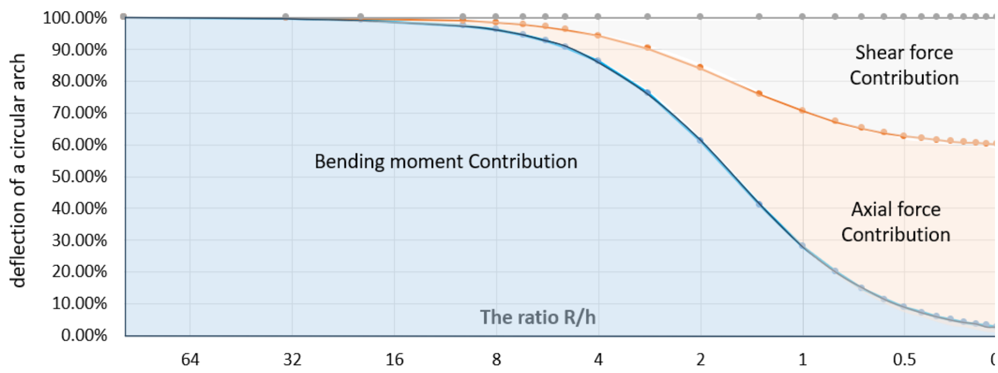

Fig. 3: Graphical dependence of the R/h ratio and the percentage contribution of internal forces to the vertical deflection.

The effect of internal forces on the total deformation is reflected in the form of strain energy. For an R/h ratio of 10, the strain energy contribution from the bending moment constitutes 97.5 % of the total. This suggests that for arches with such a ratio, the vertical deformation could be calculated analytically by considering only the first term in Equation (6). Neglecting the contributions of axial and shear forces in this case would not introduce significant. However, for lower R/h ratios, the results indicate the necessity of including the effects of axial and shear forces in manual calculations to achieve sufficient accuracy.

5 Experimental measurements

To verify the accuracy of the theoretical solution, an experimental measurement was conducted in laboratory conditions (Fig. 4) at the University of Limerick. The tested semi-circular arch (made of a low carbon steel) had a radius of R = 0.5 m and cross-sectional width of b = 0.025 m and height h = 0.020 m. The assumed material properties were a Young's modulus of E = 210 GPa and Poisson's ratio of v = 0.28.

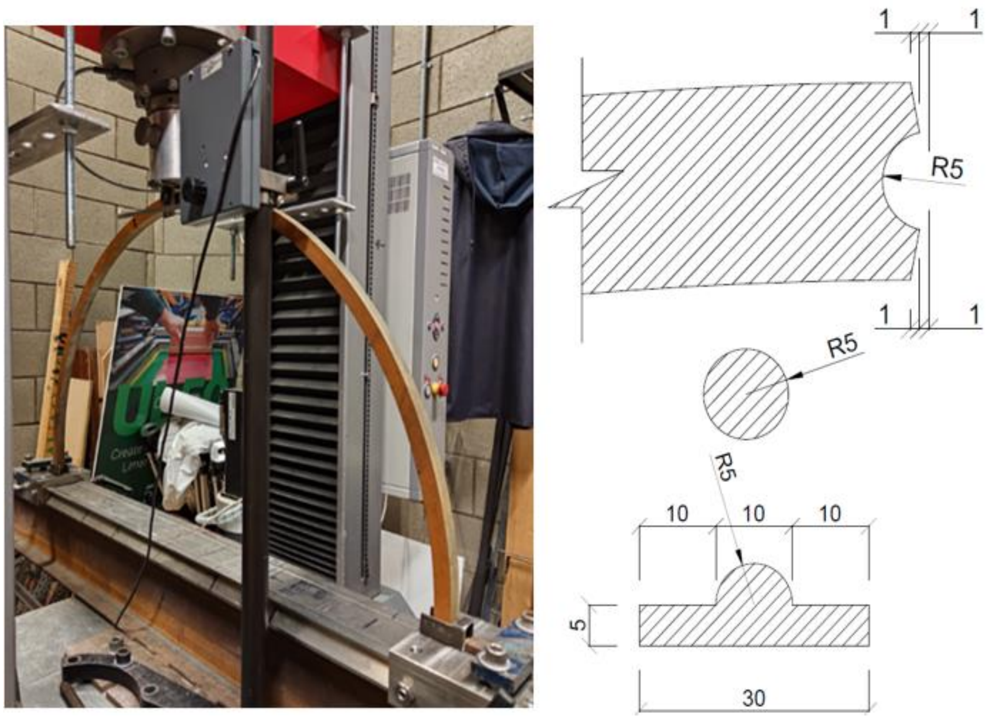

Fig. 4: Experimental measurement of the arch with a radius of 500 mm, component details.

The supports were pinned, and an apex pin was also included to yield a three-hinged arch (Fig. 1). The support points of the arch carried vertical and horizontal reactions and allowed rotation of the support, while the hinged connection at the apex of the arch was secured with a steel pin, allowing free rotation at this point. The measurement results are presented in Table 2.

Table 2: Results comparison.

R/h [-]	P [N]	ΔTheory [mm]	ΔEXP [mm]
25.36	2000	6.620	6.813

The percentage difference between the theoretical predicted apex deflection and the measured deflection was 2.92 % at a force of 2 kN.

5.1 Discussion on Further Research

The results of the presented case study provide a basis for ongoing research on secondary bending, which occurs in multilayered beam structures, both straight and curved. The secondary bending effect [1] manifests as deformations in the beams between shear blocks (Fig. 5). This phenomenon induces an additional contribution of strain energy along the beam, which subsequently leads to an increase in deflection at the arch apex.

Similarly to the presented solid model case, the Castigliano theorem can be applied to calculate the resulting deformation. However, in the case of a multilayered beam assembly, a detailed analysis of the distribution of internal forces in the regions between shear blocks is required.

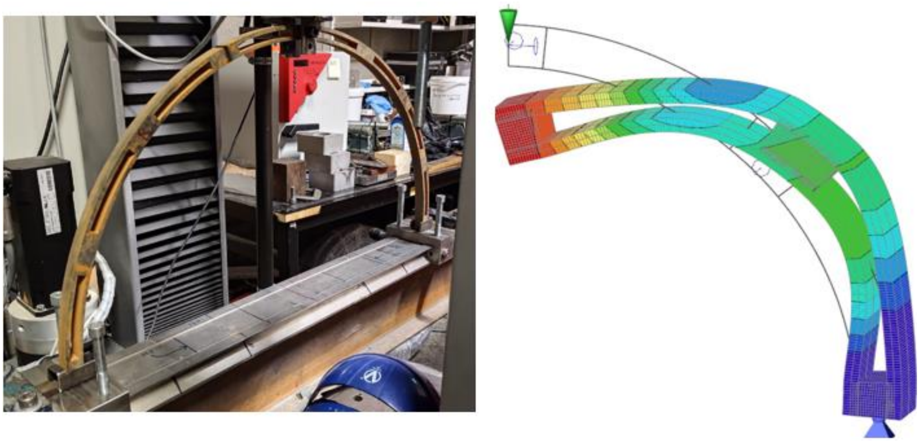

Fig. 5: Secondary bending, tests on a two-layer beam assembly.

For a proper analysis of the strain energy magnitude in a multilayered beam assembly based on Castigliano's theorem, it is essential to determine in which cases, for which parameters, and to what extent the significance of individual internal force components increases, starting with the fundamental scheme of a solid three-hinged semicircular arch.

Given the planned testing of multiple two-layer semicircular arch samples with varying numbers and positions of shear blocks, the presented case (Fig. 4) was not only used for result validation but also for assessing the design of the test setup, the hinged behaviour of supports, rotation at the apex, and potential sample tilting during the experiments.

6 Conclusion

The article presents the theoretical solution for the vertical deflection at the apex of a three-hinged semi-circular arch subjected to a point load acting at the apex. The solution also accounts for the strain energy due to axial and shear forces acting on the arch.

This study includes a parametric analysis for various R/h ratios, with results showing that for low ratios, it is necessary to include the effects of axial and shear forces in the calculation. For a ratio of R/h = 5, neglecting these effects would lead to an error of 9.28 %. All results of the theoretical study were verified using FEA models. Understanding the contribution of each term provides valuable insight into the structural behaviour, helping Engineers optimize the design.

The achieved difference between the theoretical solution for the vertical deflection of the three-hinged semi-circular arch at the apex, according to equation (6), and the experimental measurements is at most 0.24 %.

The achieved difference between the theoretical solution and experimental measurement is 2.92 %. The difference between the results can be attributed to the discrepancy between the actual material properties and the idealized material properties used in the calculation, as well as inaccuracies in the geometry along the arch caused by the water jet cutting process used to create the arch. Experimental measurement could be refined by conducting material tests [10, 11].

The results of the parametric study and experimental measurements provide insight into the contribution of individual internal forces to the overall vertical deformation of the circular arch. The presented solution could be extended to analyse non-semi-circular arches based on the relationships in [12]. However, the presented analytical solution offers a quick and practical engineering approach to preliminarily estimate the deformation of the arch and verify the size of the sections used in the construction. The use of curved elements in architecture is becoming more common. Therefore, it is necessary to focus on simplified approaches for verifying safety and dimensioning structural elements. These methods could also be applied to more complex shapes of shell structures, as discussed in [13-15]. Additionally, grid-shell structures created in a more complex manner, including active bending [16], could also benefit from such approaches. In these cases, materials other than steel, such as timber or GFRP, can be used. According to the information in [17], the use of GFRP material is also increasing today, and based on the graphical representation of Young's modulus of elasticity and flexural strength in [3], this material is considered sufficiently elastic to create curved shapes.

Acknowledgement

This paper has been supported by the Scientific Grant Agency of the Ministry of Education, science, research and sport of the Slovak Republic and the Slovak Academy of Sciences – grant VEGA 1/06377/25.

The project could also be created thanks to internal grant of Svf STU, the program for motivation and support for increasing the quality and efficiency of the scientific and research activity of young scientific and research workers 2023 – grant 1607.

References

[1] DUN, X.: An Experimental and Computational Investigation of Secondary Bending in Double Layer Gridshell Assemblies, University of Limerick, School of Engineering, Master Thesis, Limerick, 2023, 204 pp.

[2] GERE, J.M. – TIMOSHENKO, S.: Mechanics of Materials, 4th ed., Boston, MA: PWS. 1997.

[3] ASHBY, M.F.: Materials selection in mechanical design, Pergamon Press: London, ISBN 0 7506 6168 2, London, 2005, 662 pp https://ftp.idu.ac.id/wp-content/uploads/ebook/tdg/TEKNOLOGI%20REKAYASA%20MATERIAL%20PERTAHANAN/Materials%20selection%20textbook.pdf

[4] LIENHARD, J. – ALPERMANN, H. – GENGNAGEL, C. – KNIPPPERS, J.: Active bending, a review on structures where bending is used as a self-formation process, In: International Journal of Space Structures, 28(3-4), 2013, 187-196 pp. https://doi.org/10.1260/0266-3511.28.3-4.187

[5] GENGNAGEL, CH. – BÄUMER, R. – HERNÁNDEZ, E.: Natural – fibre – reinforced plastic in actively bent structures, In: Construction Materials, ISSN 1747-650X, 2013, 365-377 pp. https://doi.org/10.1680/coma.12.00026

[6] TIMOSHENKO, S.P.: Strength of Materials, Part II: Advanced theory and problems, 2 ed., D. Van Nostrand Company, 1948. https://civiltechnicalguruji.wordpress.com/wp-content/uploads/2018/07/strength-of-materials-parts-i-ii.pdf

[7] YOUNG, C.W. – BUDYNAS, G. R.: Roark´s Formulas for Stress and Strain, A division of The McGraw-Hill Companies, United States of America, ISBN 0-07-072542-X, 2002, 854 pp https://jackson.engr.tamu.edu/wp-content/uploads/sites/229/2023/03/Roarks-formulas-for-stress-and-strain.pdf

[8] TIMOSHENKO, S. P.: History of Strength of Materials. McGraw-Hill, New York, U.S.A. 1953. 231 pp. https://fst.univ-biskra.dz/images/docs/Stephen%20P%20Timoshenko-History%20of%20Strength%20of%20Materials-Dover%20Publications%20(1983).pdf
[9] BORESI, A.P. – Schmidt, R.J. – Sidebottom, O.M.: Advanced mechanics of materials, ISBN 0-471-55157-0, 827pp., United States of America, 1993.
[10] EN 10002-1: Metallic materials – Tensile testing – Part 1: Method of test at ambient temperature, European standard, 1990. 57 pp.
[11] ISO 7438: Metallic materials – Bend test, International Standard, 2016- 9 pp
[12] SONAVANE. T.: Analysis of Arches, Department of Civil, Enviromental and Architectural Engineering, Master Thesis, 2014. 160 pp. https://ceae.colorado.edu/~saouma/wp-content/uploads/pdf-files/Arches-Trupti.100eca1e.pdf
[13] HAPPOLD, E. – LIDDELL, W.I.: Timber lattice roof for the Mannheim Bundesgartenschau, In: The Institution of Structural Engineers, 1975. https://www.istructe.org/journal/volumes/volume-53-(published-in-1975)/issue-3/timber-lattice-roof-for-the-mannheim-bundesgartens/
[14] HARRIS, R. – HASKINS, S. – ROYNON, J.: The Savill Garden gridshell: design and construction, In: The Structural Engineer 86(17), ,2008, 27-34 pp. https://www.researchgate.net/publication/279585750_The_Savill_Garden_Gridshell_Design_and_Construction
[15] ROMER, J. – KELLY, O. – JOHNSON., S.: Design and construction of the Downland Gridshell, In: Building Research & Information 31(6), 2003, 427-454 pp. https://doi.org/10.1080/0961321032000088007
[16] HERDA, R. – SLIVANSKÝ, M. – SANDANUS, J.: Modeling of active bending by the method Newton-Raphson and the modified Newton-Raphson, In: Civil and Environmental Engineering, 2024, 862-870 pp. https://doi.org/10.2478/cee-2024-0063
[17] HAMED, Z.R. – HASSAN, F.H: Structural behavior of GFRP - RC slender columns under various eccentricity loading conditions, In: Civil and Environmental Engineering, 2023, 1-16 pp. https://doi.org/10.2478/cee-2023-0001